Pyrolysis of Almond Shells. Energy Applications of Fractions

Juan F. González,* Antonio Ramiro, Carmen M. González-García, José Gañán, José M. Encinar, Eduardo Sabio, and Jesús Rubiales

Departamento Ingeniería Química y Energética, UEX, Avda, Elvas s/n, 06071 Badajoz, Spain

The pyrolysis of almond shells residues were studied in nitrogen atmosphere in a laboratory fixed bed reactor. The influence of the temperature (300−800 °C) and the heating rate (5−20 K min^{-1}) on the composition and properties of the different fractions were analyzed. As the temperature was increased a decrease in the char yield and an increase in the gas yield was observed. The oil fraction yield passed through a maximum at temperatures between 400 and 500 °C. The decline at higher temperatures was likely due to the strong cracking, which increased the gas yield. The increase of the heating rate leads to a slight decrease of the char and oil yields and an increase of the gas yield. The production varied in the ranges between 21.5 and 47.3% for char, 31−51.5% for oil, and 11.4−47.5% for gas, with a maximum higher heating value of 29.0 MJ kg^{-1}, 14.1 MJ kg^{-1}, and 15.5 MJ N^{-1} m^{-3}, respectively. The char had a high fixed-carbon content (>76%) as well as a high heating value, and therefore it could be used as solid fuel, precursor in the activated carbons manufacture (specific surface area BET until 121 m^2 g^{-1}), or to obtain category-A briquettes. Aliphatic and aromatic hydrocarbons and hydroxyl and carbonyl compounds were the majority components of the oil fraction, which suggests their use as a source of chemicals of industrial interest. Also, it can be used as liquid fuel. The gas composition was identified as hydrogen, carbon monoxide, methane, and carbon dioxide and can be used to heat the pyrolysis reactor or to generate heat/electricity in a gas-turbine/vapor-turbine combined cycle.

1. Introduction

Biomass pyrolysis has received special attention since it leads to useful products and moreover contributes to diminish the environmental pollution arising from wastes accumulation and/or open field burning. Biomass use with energy aims is increasing in most countries as a clean and renewable substitute for fossil energy. One residue of this kind is almond shell, which is biodegradable. This residue is a very abundant waste product in SW Spain (Extremadura region) from the manufacture of almond sweets, 2800 t/year are generated in this region. Like most biomass residues, almond shells are composed of cellulose, hemicellulose, and lignin,[1−3] and when they heated in an inert atmosphere, they decompose into various pyrolysis products (char, gases, and oils) depending on the operating conditions (principally the temperature and the heating rate).[4−7] Pyrolysis of lignocellulosic materials is complex due to the different reactivities of their constituents. Depending on the operating conditions, different reactions associated with the thermal decomposition of each constituent occur that in turn bring about changes in material properties.[3] Interactions between constituents and traces of mineral matter present in all biomass residues, which catalyze numerous reactions that take place during pyrolysis,[1,8] introduce additional factors of complexity, making it difficult to achieve a generalized knowledge of the lignocellulosic residues pyrolysis. However, different applications for the three fractions obtained in the pyrolysis have been reported. Thus, the char is a carbon-rich nonvolatile solid residue that could be used as fuel, briquettes,[9−12] activated carbon,[3,12−15] or char-oil or char-water slurries.[12,16,17] The liquid fraction, bio-oil, has the potential to be used as a fuel-oil substitute[18−22] or may contain chemicals in economically recoverable concentrations.[4,7,21−23] The gases have a sufficiently higher heating value (HHV) to be used for the total energy requirements of a biomass waste pyrolysis plant,[16,17] to feed gas turbines in combined cycle technologies[24,25] or gas-fired engines, and fuel cells.[25] Most commercial-scale pyrolysis plants are designed to have only one of these classes as the principal product, with at least one of the other classes serving as a fuel source.[4] Thus, as example, in the Evritania (Greece) demonstration plant, the products obtained are charcoal and bio-oil, and the energy required for pyrolysis is provided by partial combustion of biomass (*Arbutus unedo*) and from its volatile components.[26]

With these antecedents, we report in this work the results obtained in the pyrolysis of almond shell residues, including the influence of the temperature and the heating rate on the composition and distribution of the different fractions. Possible applications of the different fractions are given.

2. Experimental Section

The raw material whose thermal decomposition has been studied was the almond shell residue. The material was shredded to 0.63−2.5 mm diameter particle size and was stored under dry conditions. The almond shells were dried at 110 °C for 12 h prior to the experiments.

The experiments were performed to evaluate the products obtained from the pyrolysis process, focusing on their potential energy use. A cylindrical stainless steel atmospheric pressure reactor was used, which was provided with a ceramic furnace and power source heating system, gas-feed inlets, and accessories to collect

* To whom correspondence should be addressed. Tel.: 34-924-289619. Fax: 34-924-289601. E-mail: jfelixgg@unex.es.

10.1021/ie0490942 CCC: $30.25
Published on Web 03/16/2005

liquid and gas samples. A heat exchanger at the top kept the samples at room temperature until the start of each run when a suspension system taken down a basket containing the sample. The setup has been described in detail elsewhere.[9,11,27] For each run, the basket was loaded with 10 g of the almond shell residue which was positioned in the cooling zone of the reactor, and a nitrogen flow (200 cm^3 min^{-1}) was circulated through the entire system during 1 h to purge the air of the system. Then, the heating system was switched on until the desired temperature or the heating rate was reached. In the isothermal experiments, once the desired temperature was reached the basket was placed into the heating zone, taking this moment as the initial time of the run. The thermocouple readings showed that the heating of the samples could be considered as instantaneous. In this case, a relatively fast pyrolysis can be considered. In the dynamic experiments, the basket was already placed into the heating zone at the initial time. The temperature range studied was between 300 and 800 °C in an isothermal regime. Also, dynamic experiments were performed with heating rates of 5−20 K min^{-1} until a final temperature of 800 °C. In this case, a slow pyrolysis can be considered, and the purpose of these runs is to maximize the liquid production and facilitate its recovery. Run times were 30 min for isothermal experiments, and until the final temperature was reached for the nonisothermal experiments. Gas samples were withdrawn at regular intervals. Finally, the yields of the solid and the liquid fractions were determined once the system had cooled until room temperature. The determination of hemicelluose, cellulose, and lignin of almond shell was performed by the Van Soest method using Dosi-Fiber equipment. The gas fraction composition, mainly hydrogen, carbon monoxide, methane, and carbon dioxide, was quantified using a gas chromatograph with a thermal conductivity detector and a double injector connected to two columns, one a 60/80 (mesh range) Carboxen 1000 of 15 ft × 1/8 in. stainless steel (2.1 mm i.d.) and the other a 100/120 (mesh range) Porapak Q of 3 m × 1/8 in. stainless steel (2 mm i.d.). The solid phase was characterized by proximate analysis, using an ASTM standards TGA method.[28] The solid and liquid fractions were characterized by FT-IR analysis with a Perkin-Elmer 1720 FT-IR spectrometer using samples dispersed in KBr pellets. Elemental analyses of the raw material and bio-oil were performed in a LECO corporation analyzer CHN-800 (EA 1108). The oil selected for analysis in this study was the obtained in the maximum yield. The water content of the bio-oils was determined by centrifugation and confirmed by Karl-Fisher titration. Density (at 20 °C) and viscosity (at 50 °C) of the bio-oil were determined by picnometry (norm EN 14214) and Broockfield viscosimeter model LVTD, respectively. Flash and combustion points were determined by the Cleveland method (norm UNE 51-023-90). The pour point was determined according to ASTM D97-87 and IP 15/67. Nitrogen adsorption isotherms at 77 K of the chars were determined in a semiautomatic Autosorb-1 analyzer (Quantachrome). A Parr 1351 bomb calorimeter (norm ISO 1928) was used to evaluate the HHV of the liquid and solid fractions.

3. Results and Discussion

3.1. Feedstock Characteristics. The proximate and elemental analyses, lignocellulosic composition, and the higher heating value of the almond shell residue are listed in Table 1. Comparison with the typical mean values for coals shows much higher H/C and O/C ratios, lower nitrogen and sulfur contents, much higher volatile content, and lower ash, fixed-carbon, and HHV. Also, the almond shell residues have a higher hemicellulose and cellulose content and lower lignin content than those for cherry stones.[11] These results are similar to those published by other authors for this studied residue.[29,30]

Table 1. Characteristics of the Almond Shell[a]

elemental composition (wt % daf)		proximate analysis (%)		lignocellulosic composition(%)		HHV, MJ kg^{-1}
C	50.5	fixed carbon	15.87	cellulose	37.4	18.2
H	6.58	volatiles	80.28	hemicellu.	31.2	
N	0.21	ash	0.55	lignin	27.5	
S	0.006	moisture	3.3	extractives	3.9	
O	42.654					
Cl	0.05					

[a] H/C molar ratio: 1.56; O/C molar ratio: 0.63; empirical formula: $CH_{1.56}O_{0.63}N_{0.0035}$.

3.2. Fraction Yields and Characterization of Chars. In Table 2 the fraction yields, the proximate analysis, and HHV of the chars for the isothermal and dynamic experiments are listed. The fraction yields were obtained by means of a mass balance (the liquid and solid fractions were weighted and the gas fraction detected by chromatography), and experimental errors lower than 5% with respect to the initial mass were achieved. As the temperature was increased there was a decrease in the yield of the char and an increase in the yield of gas. The liquid fraction yield passed through a maximum at temperatures between 400 and 500 °C, probably due to the strong cracking at higher temperatures. This fact suggests that the observed increase in the gas yield is partially due to the decrease in the liquid fraction. This effect was observed by us in previous works to study the pyrolysis of other lignocellulosic residues[9−11,27,31] and also by other workers.[32] Similar yields have been reported by other authors[30] for the pyrolysis at 850 °C of this kind of residue (57% of residue+tars, 43% of gases). Also, the increase of the temperature produced a slight increase in the ash content and a significant increase in the fixed carbon content of the chars. Logically, the volatile matter content of the chars decreases. In the set of dynamic experiments the increase of the heating rate leads to a slight decrease in the char and liquid fraction yields and a slight increase in the gas yield. These results agree with those reported by other workers[12] and obtained by us in previous work.[11] In this set of experiments, the liquid yield was higher than in the isothermal runs, except to for 400 °C, since the volatiles are liberated more slowly, minimizing the cracking process of the liquid fraction. The proximate analysis of the chars is not dependent on the heating rate, as it can be seen in Table 2, and is very similar to that obtained in the isothermal experiment at 800 °C (this temperature was the final temperature in the dynamic experiments). It is important to emphasize the high fixed carbon percentage of the chars, which is very interesting for their possible applications, as it will be seen below. The HHV of the chars is practically constant in this set of experiments.

Figure 1 shows the FT-IR transmittance spectra of the chars obtained in the isothermal runs performed at

Table 2. Fraction Yields, Proximate Analysis, and HHV of the Chars and HHV of the Bio-Oils

variable temp, °C	fraction yields, %			proximate analysis, %[a]			HHV MJ kg^{-1} chars	HHV[b] MJ kg^{-1} bio-oils
	char	liquid	gas	fixed carbon	volatiles	ash		
300	47.3	41.3	11.4	60.4	38.4	1.2	26.3	13.7 (23.6)
400	30.6	53.1	16.3	76.9	21.2	1.9	28.2	14.1 (23.3)
500	26.0	49.3	24.7	85.9	12.1	2.0	29.0	12.4 (24.5)
600	23.5	44.3	32.2	91.4	5.8	2.8	29.0	12.0 (24.6)
700	21.7	36.3	42.0	92.4	4.7	2.9	27.4	11.6 (24.7)
800	21.5	31.0	47.5	93.9	3.1	3.0	25.8	11.3 (24.7)
heating rate, K min^{-1}	fraction yields, %			proximate analysis, %[a]			HHV MJ kg^{-1} chars	HHV[b] MJ kg^{-1} bio-oils
	char	liquid	gas	fixed carbon	volatiles	ash		
5	26.3	51.5	22.3	94.3	3.7	2.0	29.0	12.4 (24.2)
10	24.9	50.8	24.3	95.8	2.2	2.0	28.2	12.8 (24.0)
15	22.8	50.5	26.7	95.3	2.8	1.9	28.4	13.0 (24.1)
20	22.1	49.9	28.0	93.7	3.7	2.6	28.4	13.7 (23.7)

[a] wt % on dry basis. [b] Between brackets are given the water content of bio-oils.

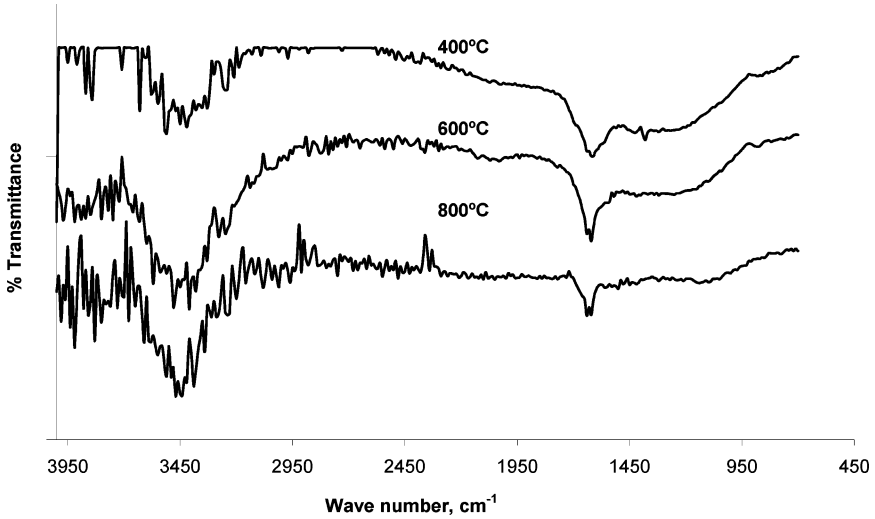

Figure 1. FT-IR transmittance spectra of the chars obtained from almond shells. Influence of the temperature.

400, 600, and 800 °C. This analysis evaluates the surface functional groups and provides information about the chemical nature and polarity. Concretely, the oxygenated groups are very important to the posterior development of porosity in a gasification process. These groups increase the solid reactivity favoring the gasification reaction. The spectra obtained for the three chars are very similar. The spectra display a number of main absorption bands located around 3450 and 1600 cm^{-1} and in the ranges between 1400 and 1600 and 950−1350 cm^{-1}. Similar spectra were obtained for the chars in the dynamic experiments. It can be seen a very intense band centered at 3450 cm^{-1}, which is related to O−H stretching vibrations ν(O−H) in water molecules. According to Zawadzki[33] a broad band below 3700 cm^{-1} is probably due to the formation of hydrogen bonds $(H_2O...H...H_2O)^+$ with superficial acid protons. The O−H stretching vibrations at 3200−3700 cm^{-1} can be assigned to hydroxyl groups (alcohols, phenols, or carboxylic acids), which seem to be the most abundant as it is reflected in the bandwidth. Also, a band localized approximately at 1600 cm^{-1}, which can be associated with vibrations in oxygenated structures, as iono radical or highly conjugated quinone C=O groups, and C=C vibrations in aromatic rings whose intensity is increased due to the presence of phenol or ether groups. Also, the bands between 1600 and 1400 cm^{-1} could be due to antisymmetric and symmetric stretchings of CO_2 ions.[34] Several overlapped bands between 1350 and 950 cm^{-1} are assigned to ν(C−O) vibrations in ether-type structures and hydroxyl groups,[35] that is, a band centered at 1260−1280 cm^{-1}, which is assigned to aromatic ether or epoxy groups, at 1210−1240 cm^{-1} corresponding to OH phenolic groups, and at 1110−1140 cm^{-1} to cyclic ethers in five- or six-membered rings.[35] The overlapping of bands in this region suggests that different oxygenated structures with C−O bond can exist in these charcoals.

In Figures 2 and 3 the adsorption isotherms of N_2 at 77 K for the chars obtained in the isothermal and dynamic series, respectively, are shown. These isotherms belong to the type I with certain tendency to type IV isotherm of the BDDT classification,[36] mainly the isothermal samples at 600 °C and 700 °C. The optimal results in the two series of experiments were obtained at 600 °C and 5 K min^{-1}. This fact can also be seen in Table 3, where the micropore and mesopore volumes (obtained from the N_2 adsorption isotherm) and the BET specific surface area (S_{BET}) are given. In these figures and Table 3, it can be seen that an increase of the temperature or the heating rate does not improve the textural properties of the chars. This fact has been observed by other authors,[13] and it can be due to a sintering effect, following by shrinkage of the char and realignment of the char structure which leads to a decrease of the mean-size and volume of the pores. Therefore, the optimal conditions of the carbonization process previous to the activation stage of these chars

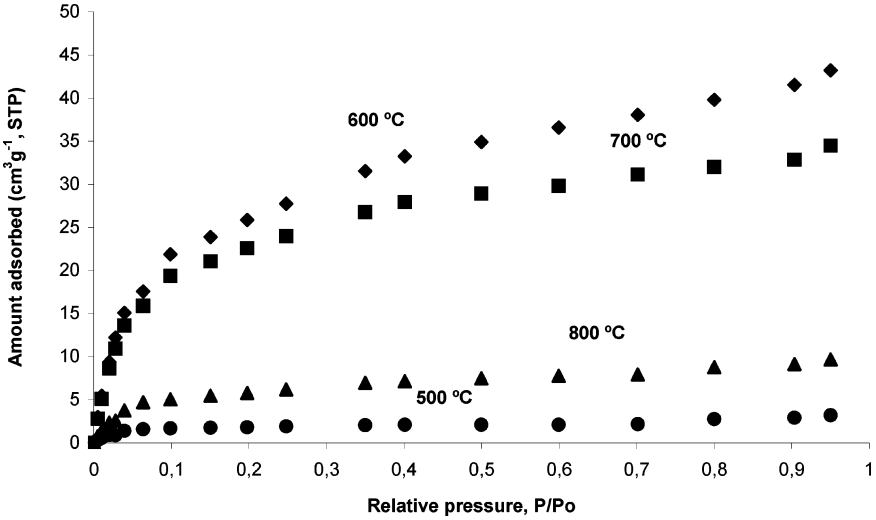

Figure 2. Nitrogen adsorption isotherms at 77 K of the chars. Influence of the temperature.

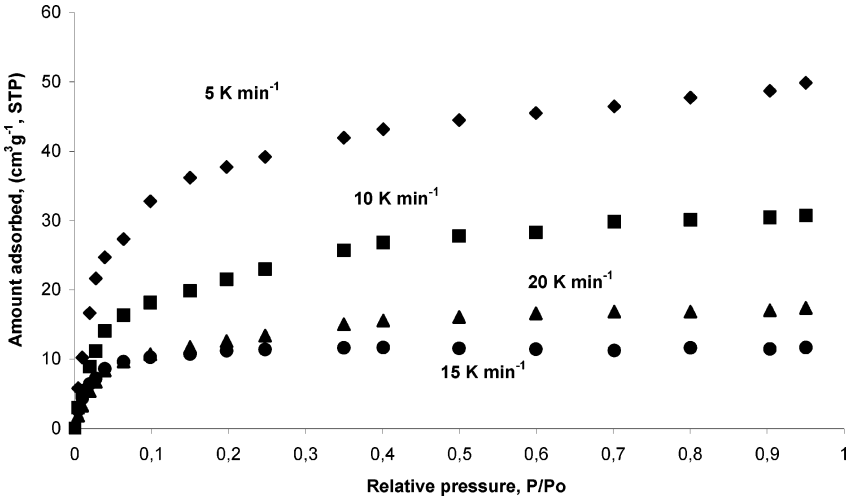

Figure 3. Nitrogen adsorption isotherms at 77 K of the chars. Influence of the heating rate.

Table 3. Micropore and Mesopore Volumes and BET Specific Surface Area of the Chars

temp, °C	V_{micro}, $cm^3\ g^{-1} \times 10^2$	V_{meso}, $cm^3\ g^{-1} \times 10^2$	S_{BET}, $m^2\ g^{-1}$
500	0.3	0.2	6
600	3.4	3.3	93
700	3.0	2.3	78
800	0.8	0.7	20
heating rate, K min^{-1}	**V_{micro}, $cm^3\ g^{-1} \times 10^2$**	**V_{meso}, $cm^3\ g^{-1} \times 10^2$**	**S_{BET}, $m^2\ g^{-1}$**
5	5.1	2.6	121
10	2.8	1.9	75
15	1.6	0.2	33
20	1.7	1.0	44

would be at temperature until 600 °C with a heating rate of 5 K min^{-1}. Marcilla et al.[37] have obtained surface area values from 4.9 to 133.1 $m^2\ g^{-1}$ for almond shell chars at 850 °C and different residence times in the pyrolysis reactor. Other authors[38] have obtained values of 1.7 and 100 $m^2\ g^{-1}$ for wood chars at 5 K min^{-1} until 350 and 850 °C, respectively, which are similar to those obtained in this work. Guo and Lua[13] have obtained higher S_{BET} values (318 $m^2\ g^{-1}$ at 850 °C and residence time of 3 h) for oil palm stones char. According to the Dubinin-Astakhov model, in Figure 4 the pore size distribution of the chars in the region of the micropores is given. As an example in the isothermal set, it can be seen that the chars have a homogeneous distribution with micropore sizes very similar. On the other hand, in the dynamic set the curves were practically overlapped.

Thus, the char with a maximum HHV of 29 MJ kg^{-1} can be used as a solid fuel, precursor in the activated carbons manufacture, and according to French and Belgian standards[39,40] and given that the fixed carbon content is higher than 76% (except to for char obtained at 300 °C) and, as raw material to make category-A briquettes for domestic use. Other workers[12] have obtained biochars with a lower HHV (27 MJ kg^{-1}) and suggest the same applications.

3.3. Bio-Oil Composition and Applications. The yield of bio-oil is high (Table 2), reflecting the potential of almond shells as a substitute for fossil fuels and a source of refined chemicals. The HHV of the liquids (Table 2) presents a maximum value at 400 °C, the same as the maximum for liquid-phase yield. This fact can be related with the cracking process that the cited phase suffers with increasing the temperature. This effect is minimized for the dynamic runs, since the HHV of bio-oils increases with increasing the heating rate. It is appreciated that the HHV of bio-oil is correlated with the water content, as it is observed in Table 2. Thus, the bio-oil obtained at 400 °C has the lowest water content. Therefore, as fossil fuel substitutes, many

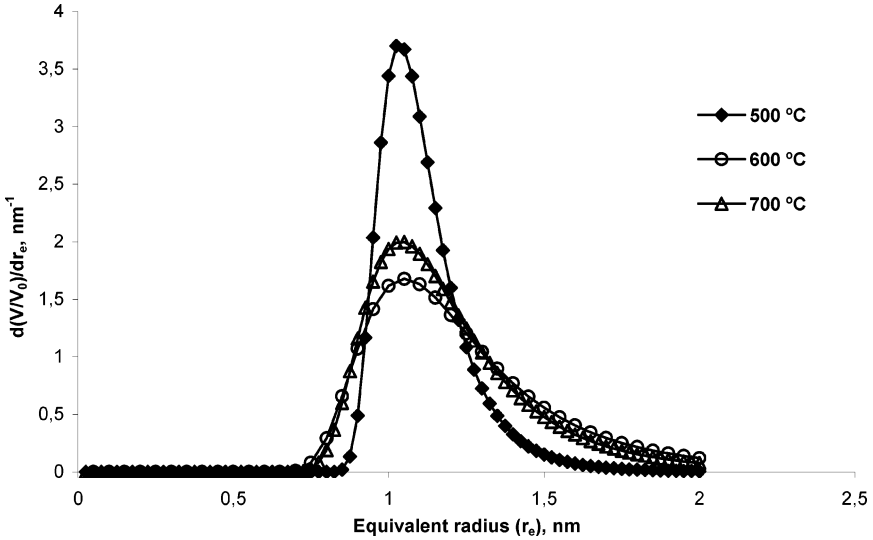

Figure 4. Pore size distribution of the chars according to the Dubinin-Astakhov model. Influence of the temperature.

Table 4. Physicochemical Properties of Different Pyrolysis Oils

analysis	almond shell oil	cherry stone oil[a]	straw oil[b]	pine oil[c]	diesel no. 2
pH	5.5	2.6	3.7	2.6	
water, wt %	22.3	26.4	19.9	21.4	1
density, kg/m^3	1106	1100	1186	1266	847
viscosity, cSt (50 °C)	1.68	1.29	11	46	<2.39
elemental composition (wt % on dry basis)					
C	48.8	46.9	55.3	56.4	86
H	6.2	7.9	6.6	6.3	11.1
N	0.3	<0.1	0.4	0.1	1
S	0.01	0.01	0.05	0.006	0.8
O (by difference)	44.7	45.1	37.7	37.2	0
Cl	0.03		0.033	0.008	
flash point, °C	110	72	56	76	85
combustion point, °C	120	78			92
pour point, °C	−15	−21	−36	−18	−23

[a] Values obtained from ref 11. [b] Values obtained from ref 47. [c] Values obtained from ref 20.

properties of these oils will have to be improved, that is, high water content, high viscosity, poor ignition characteristics, corrosiveness, and instability. However, the combustion tests performed in boilers, diesel engines, and turbines have demonstrated the possibility to use bio-oils produced from pilot plant in the present or slightly modified equipment.[18] The use of bio-oils obtained from pyrolysis as fuel for a boiler, gas turbine, and stationary diesel engines has been suggested by several authors.[41−45] For their use as liquid hydrocarbon sources it will be necessary to develop fairly expensive and complex separation methods since biomass pyro-oils are not pure hydrocarbons. Chemical characterization of the pyrolysis oils based on the fractionation of the oils by means of solvent extraction and adsorption chromatography has been utilized by several authors to identify the chemical composition.[19,20,22,46,47] Chemicals that have been reported as recovered are polyphenols for resins with formaldehyde, calcium and/or magnesium acetate for biodegradable deicers, fertilizers, levoglucosan, hydroxyacetaldehyde, and a range of flavorings and essences for the food industry.[48] Other authors[25] have explored the possibility of obtaining synthesis gas/high-Btu-value gas from the pyrolysis of the biomass-derived oil. In general, bio-oils consist of different size molecules derived from the depolymerization and fragmentation reactions of three key biomass building blocks: cellulose, hemicellulose, and lignin. Therefore, the elemental composition of bio-oil is similar to that of the biomass, as one can see in Table 4 where the bio-oil properties of the different residues are listed, including the results of this present work. One sees that the values of the almond shell bio-oil are very similar to those for the other bio-oils. In contrast to petroleum fuels, bio-oils have very high oxygen content, usually around 45−50 wt %. García et al.[30] have identified in the oils from almond shells that this oxygen is present in more than 60 compounds. The water content of the bio-oils is also very high (15−30%) compared with diesel no. 2. This content is responsible for the lower HHV of the bio-oils, as it was mentioned above, only it is obtained a 35−45% percentage of the fuels value derived of the petroleum. The HHV obtained in this work are lower than those reported by other workers for the bio-oils from other type of residues.[47] Also, because of the higher density (1106 kg m^{-3} compared with 847 kg m^{-3} for diesel) than diesel no. 2, the bio-oil heating value on a volumetric basis is about 42% of that for the diesel.

The main products from almond shell pyrolysis are condensable liquids. The single most abundant bio-oil component is water. Some compounds identified by García et al.[30] in the almond shell bio-oil are benzene, *n*-butanol, toluene, styrene, phenol, benzofuran, indene, naphthalene, methylnaphthalene, acenaphthylene, fluorene, phenanthrene, pyrene, benzofluorene, and benzofluoranthene. The quantitative analysis of the components of the bio-oils is very difficult. The FT-IR technique is not the most appropriate analytical tool to

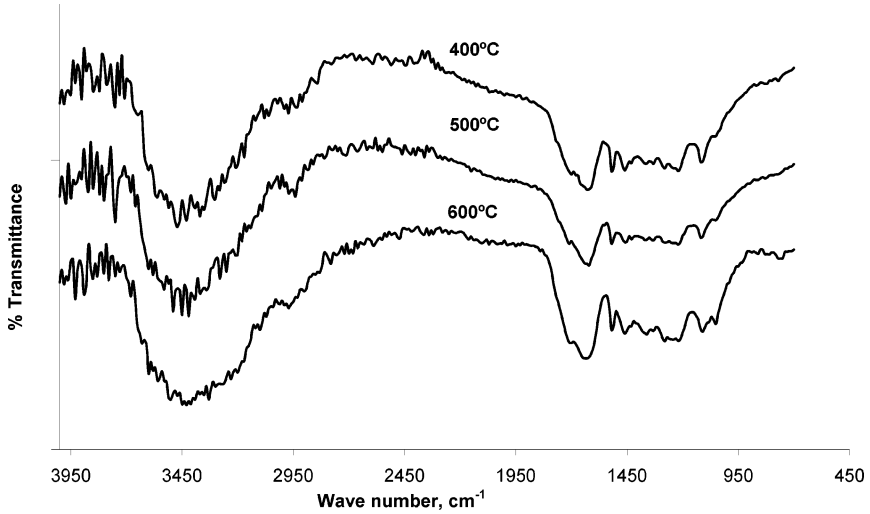

Figure 5. FT-IR transmittance spectra of the oils obtained from almond shells. Influence of the temperature.

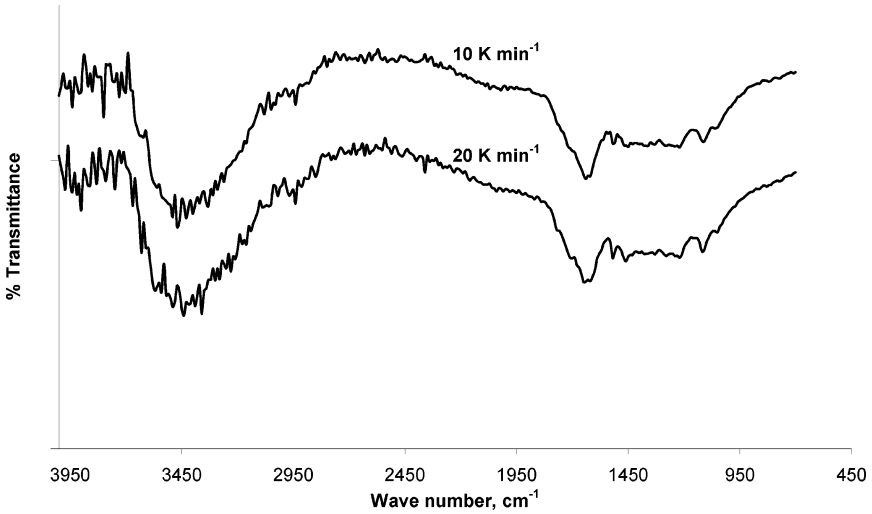

Figure 6. FT-IR transmittance spectra of the oils obtained from almond shells. Influence of the heating rate.

determine saturated, aromatic, and polar components. Nevertheless, it allows the analysis of functional groups to obtain the chemical properties of the oils. Figures 5 and 6 show the FT-IR transmittance spectra of the oils for the runs performed at 400, 500, and 600 °C and 10 and 20 K min^{-1}, respectively. In general the spectra are very similar for the two groups of experiments. The O−H stretching vibrations at 3200−3700 cm^{-1} can be assigned to hydroxyl groups (water, alcohols, phenols, or carboxylic acids), and as the bandwidth reflects these groups would be the most abundant. The aliphatic C−H stretching vibrations at 2800−3000 cm^{-1} and C−H deformation vibrations at 1350−1500 cm^{-1} indicate the presence of alkanes. The C−H stretching at 3250−3050 cm^{-1}, carbon−carbon stretching vibrations at 1600 and 1500 cm^{-1}, C−H in-plane bending between 1150 and 1000 cm^{-1}, and C−H out-of-plane bending peaks in the 900−650 cm^{-1} region indicate the presence of aromatic compounds. Furthermore, mono- and polycyclic and substituted aromatic groups are indicated by the absorption peaks between 700 and 900 and 1400−1600 cm^{-1}. The peaks between 1550 and 1750 cm^{-1} and 900−1000 cm^{-1} represent C=C stretching vibrations and are indicative of alkenes, whereas the first peaks may also be due to carbonylic groups (aldehydes or ketones, quinones). The obtained results demonstrate that the bio-oils obtained in this work would be an excellent source of chemicals of different nature and that the distribution of products is in agreement with those found by other workers.[22,46]

Table 5. Gas Production and HHV: Influence of the Temperature and the Heating Rate

variable temp, °C	gas production, mol kg^{-1} of almond shells				HHV, MJ $N^{-1}\,m^{-3}$
	H_2	CO	CH_4	CO_2	
300	0.03	1.16	0.05	1.65	5.9
400	0.11	1.91	0.43	2.73	8.3
500	0.59	3.74	1.30	3.37	11.9
600	1.54	4.61	2.18	4.06	13.4
700	3.38	6.94	3.28	4.31	14.7
800	5.84	7.25	3.94	3.96	15.5
heating rate, K min^{-1}	**gas production, mol kg^{-1} of almond shells**				**HHV, MJ $N^{-1}\,m^{-3}$**
	H_2	CO	CH_4	CO_2	
5	2.25	2.62	1.22	2.85	12.4
10	2.49	2.79	1.57	3.05	13.1
15	2.76	3.32	1.98	3.90	13.2
20	3.18	3.51	2.19	4.21	13.2

3.4. Gas Production. 3.4.1. Gas Composition. Influence of Operating Variables. In Table 5 are listed the influence of the temperature and the heating rate on the gas production and the HHV of the gas fraction. The gases were mostly H_2, CO, CH_4, CO_2 and

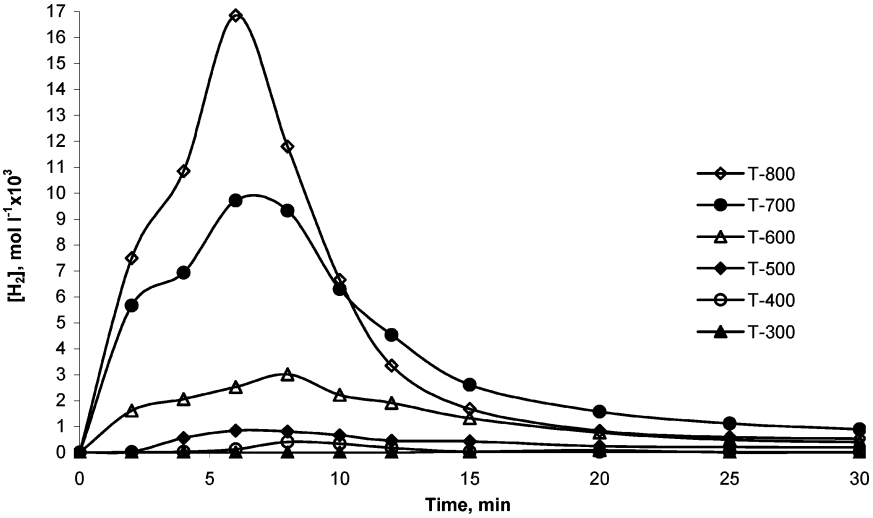

Figure 7. Temperature influence on the evolution of H_2 concentration.

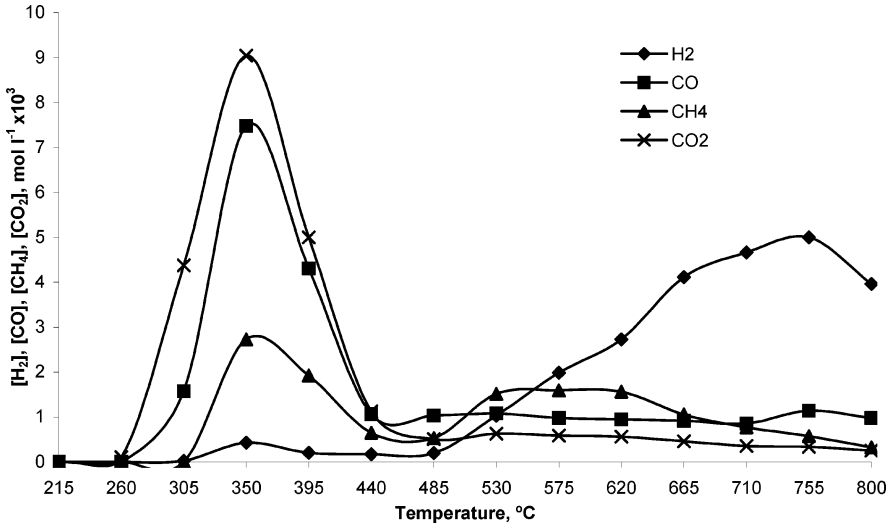

Figure 8. Evolution of H_2, CO, CO_2, and CH_4 concentration with the temperature at 10 K min^{-1}.

Table 6. Temperatures of the Maximum Generation of the Gases at Different Heating Rates

	H_2		CO		CH_4		CO_2	
heating rate, K min^{-1}	T_I, °C	T_{II}, °C	T_I, °C	T_{II}, °C	T_I, °C	T_{II}, °C	T_I, °C	T_{II}, °C
5	305	710	305	485	350	530	305	
10	350	755	350	530	350	575	350	530
15	350	755	350	665	395	620	350	665
20		755	395		440	620	350	

small traces of C_2H_2, C_2H_4, and C_2H_6. An increase of the temperature and the heating rate leads to increase practically all gases, with a concomitant increase in the HHV of the total effluent gas, lower in the dynamic runs. As it was mentioned above, this gas of low/medium heating value can be used for various applications. This gas composition has been detected by us in previous works[9−11,27,31] and by other authors in the pyrolysis of almond shells,[29,30] wood,[26] rice husks,[5] and olive stones.[49]

The generation of the main pyrolysis gases has thermal origin. Thus, hydrogen is produced by cracking of volatiles (hence its high level of production in this work above 600 °C, see Table 5). The gases CH_4, C_2H_2, C_2H_4, and C_2H_6 are produced by cracking and depolymerization reactions, and CO and CO_2, by decarboxylation and depolymerization reactions or secondary oxidation reactions of carbon.[50] These reactions are favored by increasing the temperature, leading to a greater gas production. Also, the pyrolytic gases can participate in secondary reactions which modify the outlet gas composition.[8] However, these reactions are minimized when a purge gas is used to remove the gases produced in the reaction zone,[51,52] as it was made in the present experiments. Shafizadeh[53] has reported that hemicellulose, as represented by xylan, decomposes mainly in the range between 220 and 320 °C, cellulose at 250−360 °C, and lignin undergoes gradual decomposition at 180−500 °C. Therefore, the products distribution of the almond shell pyrolysis will depend on the thermal decomposition of the majority components. In the isothermal runs it is difficult to distinguish if the produced gases correspond to the hemicellulose, cellulose, and lignin decomposition. Thus, as it can be seen in Figure 7, as with the H_2 example a unique maximum is observed in the concentration evolution of the gases versus the time. In this case, a simultaneous decomposition of the three majority components can occur.

In Figure 7 it can be seen that an increase of the temperature leads to an increase of the maximum hydrogen concentration values. Moreover, at higher temperature, the maximum gas concentration obtained is higher, and the reaction time needed to reach it is lower. It can also be deduced that the total moles of

Table 7. Comparison of Experimental Data of This Work with Other Reported Data

	almond shell (present work)	olive kernel (Zabaniotou et al.[57])	cotton gin (Zabaniotou et al.[58])	wheat straw (Zanzi et al.[59])	corn cob (Cao et al.[60])
Raw Material Characteristics (daf: Dry and Ash Free, mf: Moisture Free)					
C (wt % daf)	50.50	44.30	49.74	45.6	47.63
H (wt % daf)	6.58	5.85	6.07	6.5	4.91
N (wt % daf)	0.21	0.00	3.17	0.5	0.84
S (wt % daf)	0.006		0.00		0.14
O (wt % daf) by diff	42.654	49.85	41.02	47.4	37.72
Cl (wt % daf)	0.05				
ash (wt % mf)	0.55	3.90	13.3		6.23
moisture (wt %)	3.30	21.50	6.0		4.87
heating value (MJ/kg)	18.2	20.6	15.8		
hemicellul. (wt % mf)	31.2			27.3	
cellulose (wt % mf)	37.4			43.6	
lignin (wt % mf)	27.5			21.7	
extractives (wt % mf)	3.9			7.4	
Pyrolysis Characteristics					
reactor type	fixed bed	captive sample	captive sample	free-fall	tube-typed
particle size, dp (mm)	0.63−1.0	0.1−0.25		0.5−1.0	60 mesh
heating rate	20 K/min	∼200 K/s	∼100 K/s		30 K/min
maximum temp, °C	800	600	700	800	600
Yields (wt %)					
char	22.1	29.0	∼35.0	84.3	24.0
liquid	49.9	18.0		1.0	34.0
gas	28.0	53.0	∼75.0	14.7	42.0
Gas Composition (v/v%)					
H_2	24.3		14.1	35.0	7.5
CH_4	16.7	6.8	6.9	9.5	3.8
C_2H_4,C_2H_2				3.1	1.7
C_2H_6				0.1	
benzene				0.6	
CO_2	32.2	0.3		23.7	59.0
CO	26.8	92.9	78.0	28.0	28.0

hydrogen generated during the process (proportional to the area under the curve) increase with increasing the temperature (Table 5). The curves present a certain discontinuity at the earliest times of the reaction, easily observable at the higher temperatures, probably due to the overlap of the H_2 liberation from hemicellulose and cellulose thermal decomposition. The evolution of the other gases was similar. The gas production obtained in this work was similar to that for cherry stone pyrolysis;[11] however, the HHV values of gases were higher due to the major production of C_2H_4 and C_2H_6.

In the dynamic runs, the concentration evolution of the main gases generated differs notably to that of the isothermal runs. As an example, in Figure 8 the concentration evolution of H_2, CO, CO_2, and CH_4 versus the temperature for the run performed at 10 K min^{-1} is shown. To observe more clearly the formation trend of the gases, the run was prolonged until a final temperature of 800 °C. Two distinct zones can be observed: CO, CH_4, CO_2 and lower concentrations of H_2 at low temperatures between 260 and 440 °C, and H_2 and CH_4 and lower concentrations of CO and CO_2 and other hydrocarbons at temperatures higher than 450 °C. The peaks of gas evolution tended to merge as the heating rate was increased. These results have been also observed by other workers.[5] On the other hand, it can be observed that there are two maximum in the hydrogen curve: a smaller one at 350 °C than that at 755 °C. There are also two maximum in the CH_4 curves around 350 °C and 530−575 °C, and for CO and CO_2 a well-differentiated maximum at 350 °C and other smaller peak at 500−530 °C. The production of these four gases continues (mainly H_2 production) at 800 °C, as it can be seen in Figure 8. These facts have been also observed in the cherry stones pyrolysis.[11] These double maximum may correspond to the thermal decomposition of the hemicellulose and cellulose (first peak) and lignin (second peak), since the thermal decomposition of lignin begins at 200 °C and is prolonged until 500−600 °C.

According to some hypotheses, the behavior of almond shells in the decomposition process should be the sum of lignin and holocellulose multiplied by their weight fractions in the raw material. However, Caballero et al.[29] in studying the pyrolysis of almond shells have found a very good correlation in the case of water, CO_2, and CO, indicating that the separation process does not alter the formation of these products. The yields of other hydrocarbons were very different, indicating that the interactions between fractions can occur.

The release of CO and CO_2 observed during almond shells pyrolysis can be due to hemicellulose degradation at low temperatures (up to 300 °C), and cellulose decomposition leads to a maximum at 350 °C. This fact has been also reported by other authors to study the olive stones pyrolysis.[49] The cellulose degradation starts with the intramolecular dehydration to form anhydrocellulose at 220 °C, taking part with the formation of levoglucosan at 280 °C.[8] Between 240 and 400 °C large quantities of tar, water, CO, and CO_2 are due to the rupture of C−C and C−O bonds.[54] CO_2 is formed by the rupture of the glucosidic linkage and C−O bonds in the pyran ring, and CO and water from keto and primary alcohol groups. The origin of CO_2 and CO with a maximum at 350 °C is believed to be mainly due to hemicellulose and cellulose.[5] The evolution of CO and CO_2 at higher temperatures can be due to lignin,[55] possibly through the release of COOH groups and/or rupture of C−O groups, producing also water. The formation of CH_4 and other light hydrocarbons could be related to the degradation of lignin. The formation of methane is due to the release of methoxy groups, involving the rupture of C−C bonds, and it is controlled

by hydrogen transfer reactions.[56] During lignin pyrolysis, a second formation of CH_4 (as in this work occurs) above 500 °C can be due to the charring process (increase in aromaticity/cross-linking)[55] along the volatilization of aliphatic and aromatic carbons.[56] H_2 and low concentrations of C_2H_2, C_2H_4, and C_2H_6 were detected at the higher temperatures probably corresponding to the lignin decomposition and second stage of cellulose decomposition.[5]

The influence of the heating rate on the gas concentration evolution can be appreciated in Table 6, which gives the temperatures T_I and T_{II}, at which the said two maximum occur. In general, as the heating rate increases the maximum shifts toward higher temperatures. Also, an increase in the heating rate produces a larger maximum value. Thus, the area under the curve increases and therefore the gas production. This can be seen in Table 5, where the gas production and HHV of the effluent gas versus the heating rate are presented. Some workers[5] have obtained HHV values of the effluent gases from the pyrolysis of rice husks of 12.2 and 14.4 MJ N^{-1} m^{-3} at heating rates of 5 and 20 K min^{-1}, respectively, which are very similar to those obtained in the present work. Compared with the results obtained from the cherry stone pyrolysis,[11] the production of the four majority gases (H_2, CO, CH_4, and CO_2) was slightly higher in the case of almond shell and the production of light hydrocarbons (C_2H_4 and C_2H_6) is much higher in the case of cherry stone. This fact is due to the different lignocellulosic composition of the two residues.

Finally, in Table 7, the results obtained in this work are compared with those obtained by other workers in the pyrolysis of other lignocellulosic residues. One can see that the results presented in this table are clearly dependent on the residue type.

4. Conclusions

The pyrolysis of almond shells gave major recoveries of liquid hydrocarbons, solid char, and gases. As the temperature was increased, the yield of char and gas was decreased and increased, respectively. The oil fraction yield passed through a maximum at 400−500 °C. The decline at higher temperatures was likely due to strong cracking which leads to an increase in the gas yield. The heating rate produced a slight decrease in the oil and the char fraction and a slight increase in the gas fraction.

The char, with a mean HHV of 29 MJ kg^{-1}, S_{BET} until 121 m^2 g^{-1}, and high content of fixed carbon (>76%) could be used as solid fuel, precursor in activated carbons manufacture, or to make category-A briquettes. Moreover, the FT-IR analysis of chars reveals that they contained oxygenated surface functional groups, which are very important in the gasification process to carry out the activation phase. The FT-IR analysis of the oil fraction reveals that it is a mixture of aliphatic and aromatic hydrocarbons and hydroxyl and carbonylic compounds. It could be used as a source of refined chemicals or liquid fuel with a HHV in the range between 11.3 and 14.1 MJ kg^{-1}. The gas fraction consisted of H_2, CO, CH_4, and CO_2 with a HHV value up to 15.5 MJ N^{-1} m^{-3}.

Finally, the study of the variation of temperature and heating rate allows for driving the almond shell pyrolysis process in order to maximize some of the fractions.

Acknowledgment

The authors would like to express their gratitude to the "Ministerio de Ciencia y Tecnología" for the financial support through projects FIT-120100-2003-114 and PPQ2003-07268.

Literature Cited

(1) Antal, M. J.; Varhegyi, G. Cellulose Pyrolysis Kinetics. The Current State of Knowledge. *Ind. Eng. Chem. Res.* **1995**, *34*, 703−717.

(2) Liou, T. H.; Chang, F. W.; Lo, J. J. Pyrolysis of Acid-Leached Rice Husk. *Ind. Eng. Chem. Res.* **1997**, *36*, 568−573.

(3) Bonelli, P. R.; Della Roca, P. A.; Cerrella, E. G.; Cukierman, A. L. Effect of Pyrolysis Temperature on Composition, Surface Properties and Thermal Degradation Rates of Brazil Nut Shells. *Bioresour. Technol.* **2001**, *76*, 15−22.

(4) Balci, S.; Dogu, T.; Yücel, H. Pyrolysis of Lignocellulosic Materials. *Ind. Eng. Chem. Res.* **1993**, *32*, 2573−2579.

(5) Williams, P. T.; Besler, S. The Pyrolysis of Rice Husks in a Thermogravimetry Analyser and Static Batch Reactor. *Fuel* **1993**, *72*, 151−159.

(6) Antal, M. J. In *Advances in Solar Energy*; Boer, K., Duddie, J., Eds.; American Solar Energy Society, Plenum: New York, 1985; Vol. 2, pp 175−255.

(7) Bridgwater, A. V.; Evans, G. D. *An Assessment of Thermochemical Conversion Systems for the Processing Biomass and Refuse;* Report to UK DTI; 1993; p 254 (ETSU B/T1/00207).

(8) Caballero, J. A.; Conesa, J. A.; Font, R.; Marcilla, A. Pyrolysis Kinetic of Almond Shells and Olive Stones Considering their Organic Fractions. *J. Anal. Appl. Pyrolysis* **1997**, *42*, 159−175.

(9) Encinar, J. M.; Beltrán, F. J.; Bernalte, A.; Ramiro, A.; González, J. F. Pyrolysis of Two Agricultural Residues: Olive and Grape Bagasse. Influence of particle size and temperature. *Biomass Bioenergy* **1996**, *11* (5), 397−409.

(10) Encinar, J. M.; Beltrán, F. J.; González, J. F.; Moreno, M. J. Pyrolysis of Maize, Sunflower, Grape and Tobacco Residues. *J. Chem. Technol. Biotech.* **1997**, *70*, 400−410.

(11) González, J. F.; Encinar, J. M.; Canito, J. L.; Sabio, E.; Chacón, M. Pyrolysis of Cherry Stones: Energy Uses of the Different Fraction and Kinetic Study. *J. Anal. Appl. Pyrolysis* **2003**, *67*, 165−190.

(12) Karaosmanoglu, F.; Isigigür-Ergüdenler, A.; Sever, A. Biochar from the Straw-Stalk of Rapeseed Plant. *Energy Fuels* **2000**, *14*, 336−339.

(13) Guo, J.; Lua, A. C. Characterization of Chars Pyrolysed from Oil Palm Stones for the Preparation of Activated Carbons. *J. Anal. Appl. Pyrolysis* **1998**, *46*, 113−125.

(14) Mackay, D. M.; Roberts, P. V. The Influence of Pyrolysis Conditions on Yield and Microporosity of Lignocellulosic Chars. *Carbon* **1984**, *20* (2), 95−101.

(15) Keirsse, H.; Hartoyo, W.; Buekens, A.; Schoeters, J.; Janssens, J. In *Research in Thermochemical Biomass Conversion*; Bridgwater, A. V., Kuester, J. L., Eds.; Elsevier Applied Science: London, 1988.

(16) Bridgwater, A. V. In *Biomass for Energy and Industry*; Grassi, G., Gosse, G., Dos Santos, G., Eds.; Elsevier Applied Science: London, 1990.

(17) Bridgwater, A. V. In *Pyrolysis and Gasification;* Ferrero, G. L., Maniatis, K., Buekens, A., Bridgwater, A. V., Eds.; Elsevier Applied Science: London, 1989.

(18) Oasmaa, A.; Czernik, S. Fuel Oil Quality of Biomass Pyrolysis Oils-State of the Art for the End User. *Energy Fuels* **1999**, *13*, 914−921.

(19) Oasmaa, A.; Kuoppala, E.; Gust, S.; Solantausta, Y. Fast Pyrolysis of Forestry Residue. 1. Effect of Extractives on Phase Separation of Pyrolysis Liquids. *Energy Fuels* **2003**, *17*, 1−12.

(20) Oasmaa, A.; Kuoppala, E.; Gust, S.; Solantausta, Y. Fast Pyrolysis of Forestry Residue. 2. Physicochemical Composition of Product Liquid. *Energy Fuels* **2003**, *17*, 433−443.

(21) Piskorz, J.; Majerski, P.; Radlein, D.; Scott, D. S.; Bridgwater, A. V. Fast Pyrolysis of Sweet Sorghum Bagasse. *J. Anal. Appl. Pyrolysis* **1998**, *46*, 15−29.

(22) Gerçel, H. F. Production and Characterization of Pyrolysis Liquids from Sunflower-Pressed Bagasse. *Bioresour. Technol.* **2002**, *85*, 113−117.

(23) Diebold, J.; Milne, T. A. In *Pyrolysis Oils From Biomass, Producing, Analysing and Upgrading*; American Chemical Society: Washington, 1988.

(24) Williams, R. H.; Larson, E. D. Advanced Gasification-Based Biomass Power Generation. In *Renewable Energy*; Johanson, T. B., Kelly, H., Reddy, A. K. N., Williams, R. H., Eds.; Island Press: Washington, DC, 1993; pp 729−787.

(25) Panigrahi, S.; Chaudhari, S. T.; Bakhshi, N. N.; Dalai, A. K. Production of Synthesis Gas/High-Btu Gaseous Fuel from Pyrolysis of Biomass-Derived Oil. *Energy Fuels* **2002**, *16*, 1392−1397.

(26) Zabaniotou, A. A.; Karabelas, A. J. The Evritania (Greece) Demonstration Pplant of Biomass Pyrolysis. *Biomass Bioenergy* **1999**, *16*, 431−445.

(27) Encinar, J. M.; Beltrán, F. J.; Ramiro, A.; González, J. F. Catalysed Pyrolysis of Grape and Olive Bagasse. Influence of Catalyst Type and Chemical Treatment. *Ind. Eng. Chem. Res.* **1997**, *36*, 4176−4183.

(28) Valenzuela, C.; Bernalte, A. Un método termogravimétrico rápido para análisis inmediato de carbón. *Bol. Geol. Min.* **1985**, *96(1)*, 58−61.

(29) Caballero, J. A.; Font, R.; Marcilla, A. Comparative Study of the Pyrolysis of Almond Shells and their Fractions, Holocellulose and Lignin. Product Yields and Kinetics. *Thermochim. Acta* **1996**, *276*, 57−77.

(30) García, A. N.; Esperanza, M. M.; Font, R. Comparison between Products Yields in the Pyrolysis and Combustion of Different refuse. *J. Anal. Appl. Pyrolysis* **2003**, *68−69*, 577−598.

(31) Encinar, J. M.; González, J. F.; González, J. Fixed-Bed Pyrolysis of *Cynara Cardunculus L.* Products Yields and Composition. *Fuel Process. Technol.* **2000**, *68*, 209−222.

(32) van Heek, K. H.; Strobel, B. O.; Wanzl, W. Coal Utilization Processes and their Applications to Waste Recycling and Biomass Conversion. *Fuel* **1994**, *73*, 1135−1143.

(33) Zawadzki, J. IR Spectroscopic Investigations of the Mechanism of Oxidation of Carbonaceous Films with HNO_3 Solution. *Carbon* **1980**, *18*, 281−285.

(34) Pasto, D. J.; Johnson, C. R. *Organic Structure Determination*; Prentice-Hall: Englewood Cliffs, NJ, 1969.

(35) González-Martín, M. L.; Valenzuela-Calahorro, C.; Gómez-Serrano, V. Characterization Study of Carbonaceous Materials. Calorimetric Heat of Adsorption of *p*-Nitrophenol. *Langmuir* **1994**, *10*, 844−854.

(36) Brunauer, S.; Deming, L. S.; Deming; W. E.; Teller, E. J. On a Theory of the van der Waals Adsorption of Gases. *J. Am. Chem. Soc.* **1940**, *62*, 1723−1732.

(37) Marcilla, A.; García-García, S.; Asensio, M.; Conesa, J. A. Influence of Thermal Treatment Regime on the Density and Reactivity of Activated Carbons from Almond Shells. *Carbon* **2000**, *38*, 429−440.

(38) Della-Roca, P. A.; Cerrella, E. G.; Bonelli, P. R.; Cukierman, A. L. Pyrolysis of Hardwoods Residues: on Kinetics and Chars Characterization. *Biomass Bioenergy* **1999**, *16*, 79−88.

(39) Association Francaise de Normalisation, Charbon de Bois et Briquettes de Charbon de Bois á Usage Domestique: Denomination, Spécifications, Essais. AFNOR 84361 NF B 55-101, 1985.

(40) Institute Belge Normalisation (IBN), Charbon de Bois et Briquettes de Charbon de Bois á Usage Domestique: Denomination, Spécifications, Essais. NBN M 11-001, 1984.

(41) Jay, D. C.; Rantanen, O.; Spilä, K.; Nylumd, N. Wood Pyrolysis Oil for Diesel Engines. In *Proceedings of the 1995 Fall Technical Conference*, Milwaukee, Wisconsin, ASME, Internal Combustion Engine Division: New York, 1995.

(42) Toft, A. A comparison of Integrated Biomass to Electricity Systems, Ph.D. Dissertation, Aston University, Birminghan, 1996.

(43) Gust, S. In Combustion of Pyrolysis Liquids; In *Biomass Gasification and Pyrolysis, State of the Art and Future Prospects*; Kaltschmitt, M.; Bridgwater, A., Eds.; CPL Press: Newbury, UK, 1997.

(44) Andrews, R.; Fuleki, D.; Zukowski, S.; Patnaik, P. Results of Industrial Gas Turbine Tests Using a Biomass-Derived Fuel. In *Proceedings of the Third Biomass Conference of the Americas*, Overend, R., Chornet, E., Eds.; Elsevier Science Ltd.: New York, 1997.

(45) Östman, A.; Lindman, E.; Solantausta, Y.; Beckman, D. A. Comparison of Using Wood Pellets and Fast Pyrolysis Liquid Industrially for Heat Production within Stockholm. In *Progress in Thermochemical Biomass Conversion*; Bridgwater, A. V., Ed.; Blackwell Science: Oxford, 2001; Vol. 1, pp 867−874.

(46) Yorgun, S.; Şensöz, S.; Koçkar, Ö. M. Characterization of the Pyrolysis Oil Produced in the Slow Pyrolysis of Sunflower-Extracted Bagasse. *Biomass Bioenergy* **2001**, *20*, 141−148.

(47) Sipilä, K.; Kuoppala, E.; Fagernäs, L.; Oasmaa, A. Characterization of Biomass-Based Flash Pyrolysis Oils. *Biomass Bioenergy* **1998**, *14*, 103−113.

(48) Bridgwater, A. V. Principles and Practice of Biomass Fast Pyrolysis Processes for Liquids. *J. Anal. Appl. Pyrolysis* **1999**, *51*, 3−22.

(49) Blanco, M. C.; Blanco, C. G.; Martínez-Alonso, A.; Tascón, J. M. D. Composition of Gases Released during Olive Stones Pyrolysis. *J. Anal. Appl. Pyrolysis* **2002**, *65*, 313−322.

(50) Shafizadeh, F. *Adv. Carbohydr. Chem.* **1968**, *23*, 419−474.

(51) Beaumont, O.; Schwob, Y. Influence of Physical and Chemical Parameters on Wood Pyrolysis. *Ind. Eng. Chem. Process Des. Dev.* **1984**, *23*, 637−641.

(52) Helt, J. E.; Agrawal, R. K. In *Pyrolysis Oils from Biomass: Producing, Analyzing and Upgrading*; Soltes, J., Milne, T. A., Eds.; American Chemical Society; Washington, 1988.

(53) Shafizadeh, F. In *Fuels from Waste*; Anderson, L. L., Tillman, D. A., Eds.; Academic Press: New York, 1977.

(54) Fitzer, E.; Mueller, K.; Schaeffer, W. In *Chemistry and Physics of Carbon*; Walker, P. L., Jr., Ed.; Marcel Dekker: New York, 1971; Vol. 7, pp 237−383.

(55) Jagtoyen, M.; Derbyshire, F. Activated Carbons from Yellow Poplar and White Oak by H_3PO_4 Activation. *Carbon* **1998**, *36*, 1085−1097.

(56) Jakab, E.; Faix, O.; Till, F. Thermal decomposition of Milled Wood Lignins Studied by Thermogravimetry/Mass Spectrometry. *J. Anal. Appl. Pyrolysis* **1997**, *40−41*, 171−186.

(57) Zabaniotou, A. A.; Kalogiannis, G.; Kappas, E.; Karabelas, A. J. Olive residues (cuttings and kernels) rapid pyrolysis product yields and kinetics. *Biomass Bioenergy* **2000**, *18*, 411−420.

(58) Zabaniotou, A. A.; Roussos, A. I.; Koroneos, C. J. A laboratory study of cotton gin waste pyrolysis. *J. Anal. Appl. Pyrolysis* **2000**, *56*, 47−59.

(59) Zanzi, R.; Sjöström, K.; Björnbom, E. Rapid pyrolysis of agricultural residues at high temperature. *Biomass Bioenergy* **2002**, *23*, 357−366.

(60) Cao, Q.; Xie, K.-C.; Bao, W.-R.; Shen, S.-G. Pyrolytic behaviour of waste corn cob. *Bioresour. Technol.* **2000**, *94*, 83−89.

Received for review September 16, 2004
Revised manuscript received January 18, 2005
Accepted February 16, 2005

IE0490942